

# Electromagnetic-Structural Analysis of a Superconducting Magnet With Active Shielding for a Rotating Gantry

journal or publication title	IEEE Transactions on Applied Superconductivity
volume	32
number	6
page range	1-4
year	2022-03-01
NAIS	13207
URL	<a href="http://hdl.handle.net/10655/00013171">http://hdl.handle.net/10655/00013171</a>

doi: 10.1109/TASC.2022.3155535



# Electromagnetic-structural analysis of a superconducting magnet with active shielding for a rotating gantry

T. Obana

**Abstract**— As a magnet utilized for a rotating gantry in heavy particle radiotherapy, a superconducting magnet with active shielding has been proposed to reduce the magnet weight. The magnet is composed of a dipole coil and an active shielding coil wound with NbTi wires. In this study, an electromagnetic-structural analysis of the magnet with active shielding was conducted using an FEM model. The results of the analysis indicate that the coil deformation, due to an electromagnetic force, slightly affects the field quality but negligible for the operation. The design concept of superconducting magnets with active shielding is valid in terms of magnetic field and the support structure for a rotating gantry.

In addition, based on the previous study, the weight of the superconducting magnet with active shielding was reevaluated. As a result, the superconducting magnet with active shielding can be one-third lighter than a superconducting magnet surrounded with an iron yoke, in terms of the magnet weight per unit length.

**Index Terms**— Heavy particle radiotherapy, rotating gantry, electromagnetic-structural analysis, FEM model, active shielding, weight evaluation.

## I. INTRODUCTION

**I**N heavy particle radiotherapy, a rotating gantry enables charged particles to be delivered to a tumor with great accuracy. Therefore, cancer therapy that minimizes unnecessary damage to a patient can be realized by using the rotating gantry. In 2015, the world's first rotating gantry composed of superconducting magnets was developed in the National Institutes for Quantum Science and Technology [1]-[3]. Using superconducting magnets instead of conventional magnets, it became possible to make a smaller, lighter gantry [4].

A superconducting magnet for the rotating gantry is composed of a cosine-theta superconducting coil surrounded with an iron yoke which is the heaviest part of the magnet. The weight of one superconducting magnet reaches several tons, and the rotating gantry is equipped with ten superconducting magnets. Precise rotation control is required under the condition that several tens of tons are mounted on the frame of the rotating gantry. In this study, a superconducting magnet, composed of an active shielding coil for the gantry, has been pro-

posed to simplify the control system and the frame structure of the rotating gantry by reducing its weight [5]. By using an active shielding coil instead of an iron yoke to shield the stray magnetic field, the magnet's weight can be reduced.

The previous study [5] indicated the possibility that the superconducting magnet with active shielding could significantly reduce the magnet weight, compared to the superconducting magnet with an iron yoke. However, the support structure of the superconducting magnet with active shielding was not taken into account in the previous study. Considering the coil support structure, hence the design study of the superconducting magnet with active shielding was conducted based on the coil cross-section designed in the previous study. In this paper, the electromagnetic-structural analysis of the superconducting magnet with active shielding is described. Additionally, the weight of the magnet is evaluated, and the effect of the coil deformation on the field quality is discussed.

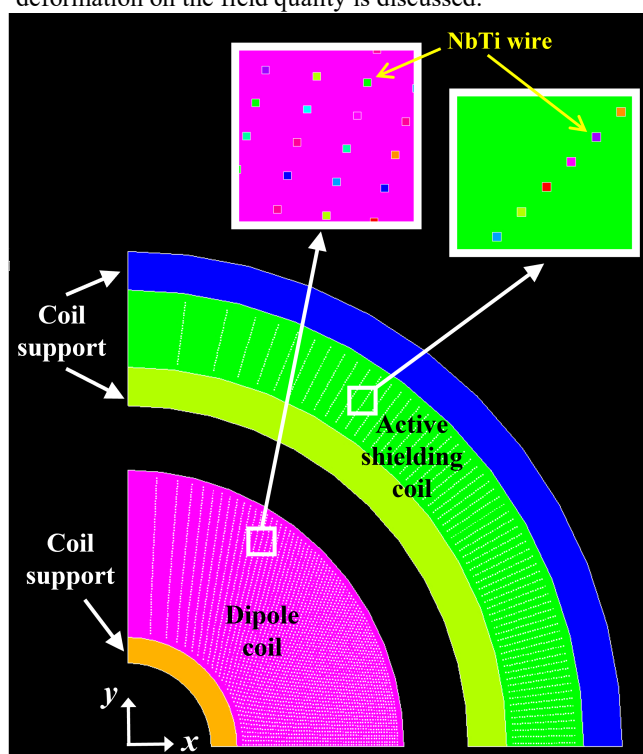


Fig. 1. The cross-section of a superconducting magnet with active shielding in the first quadrant. This cross-section is used as the FEM model for the structural analysis.

Manuscript receipt and acceptance dates will be inserted here. This work was supported by JSPS KAKENHI Grant Number JP19K04364. (Corresponding author: Tetsuhiro Obana.)

T. Obana is with the National Institute for Fusion Science, 509-5292, Japan (e-mail: obana.tetsuhiro@nifs.ac.jp).

## II. MAGNET DESIGN REQUIREMENTS

As the design requirements of the superconducting magnet with active shielding, the following requirements have been determined [5].

- (1) The inner radius of the dipole coil is fixed at 0.09 m.
- (2) The dipole field is 2.37 T in the reference radius of 0.06 m.
- (3) Higher multi-pole components normalized by the dipole component are less than  $1.0 \times 10^{-3}$ .
- (4) The stray field is less than 5 G ( $=5.0 \times 10^{-4}$  T) at a distance 0.5 m radially from the magnet center.
- (5) The load factor (= operating current /critical current) of the magnet is less than 70% at 5 K.
- (6) A superconducting wire with NbTi filaments is used for the coil winding based on the surface winding technology [6]-[8]. The diameter of the wire is 0.9 mm.

To fulfill the design requirements, the coil cross-section of the superconducting magnet has been designed [5]. The superconducting magnet is composed of the dipole coil and the active shielding coil, as illustrated in Fig. 1. The details of the coils are listed in Table 1. Regarding the material of the coil support structure, 5083 aluminum alloy is used.

Table 1. Details of the dipole coil and the active shielding coil.

	Dipole coil	Active shielding coil
Inner radius	90 mm	300 mm
Outer radius	210 mm	350 mm
Layers	60	25
Turn	6954	3000
Operating current	217 A	249 A

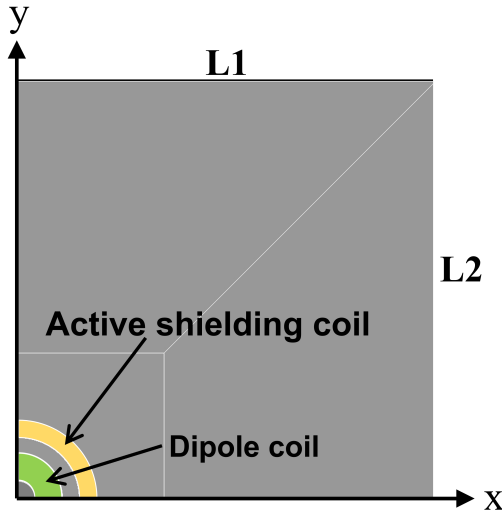


Fig. 2. Schematic view of the model for electromagnetic analysis. The wire positions of the dipole coil and the shielding coil are illustrated in Fig. 1. The infinite boundary condition is set on the lines L1 and L2 of the air.

## III. DETAILS OF FEM MODEL

The FEM model for electromagnetic analysis is composed of the air and superconducting wires for the dipole and active shielding coils, as illustrated in Fig. 2. The wire position of the dipole and the shielding coils are shown in Fig. 1. The cross-section of the superconducting wire is square the size of which

is  $0.5 \text{ mm} \times 0.5 \text{ mm}$ , instead of 0.9 diameter circle to simply the model. Regarding the boundary condition of the electromagnetic analysis, the Neumann boundary condition is set on the x-axis and the Dirichlet boundary condition is set on the y-axis, respectively. In addition, the infinite boundary condition is set on the lines L1 and L2 of the air in the model. The permeability of the wire and the air are given as vacuum permeability.

The FEM model for structural analysis of the magnet is shown in Fig. 1. The model is composed of NbTi superconducting wires, epoxy resin for coil winding, and coil support structures made of 5083 aluminum (Al) alloy. The size of the coil supports for the dipole and the shielding coils is listed in Table 2. Young's modulus and Poisson's ratio of each component are listed in Table 3. Fig. 3 shows the schematic view of the boundary conditions in the magnet cross-sectional model for structural analysis. Regarding the boundary conditions, line 4 and line 5, which are located on the x-axis, do not displace in the y-axis direction. Also, line 1 and line 2, which are located on the y-axis, do not displace in the x-axis direction. Line 3 and line 6, which are the innermost of the coil support, are fixed. The boundaries between the superconducting wires and the epoxy resin are glued. The contact element is used at the boundary between the support structure and the epoxy resin, and the coefficient of friction of the boundary is set as 0. In the study, ANSYS 19 [9], which is the commercial FEM software, was utilized for the analyses.

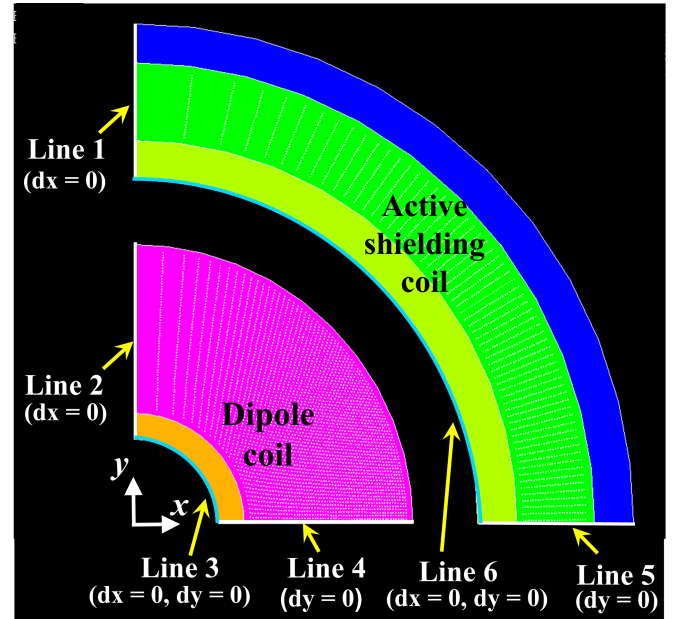


Fig. 3. The schematic view of the boundary conditions in the magnet cross-sectional model for structural analysis.

## IV. ELECTROMAGNETIC ANALYSIS

To obtain an electromagnetic (EM) force occurring in each superconducting wire in the coil winding, the electromagnetic analysis of the magnet was conducted with the FEM model illustrated in Fig. 2. Fig. 4 shows the magnetic field distribution of the magnet with active shielding at the rated operation.

There is a large gradient of the magnetic field distribution inside the dipole coil winding. Especially in the part of the coil winding attached to x-axis, the magnetic field at the inner and outer layers of the coil winding becomes larger, while the magnetic field at the middle of the dipole coil winding is very small. The peak field of the magnet is 2.46 T, which is located at the outer of the dipole coil. In this magnet, the magnitude of the peak field is comparable with that of the required dipole field. Regarding the field quality for the magnet, the details are described in Ref [5].

Table 2. Size of coil supports for the dipole and the shielding coils.

	Inner radius	Outer radius
Inner support for dipole coil	65 mm	85 mm
Inner support for shielding coil	265 mm	295 mm
Outer support for shielding coil	355 mm	385 mm

Table 3. Young's modulus and Poisson's ratio of each component for the model.

	Young's modulus	Poisson's ratio
NbTi wire	108 GPa	0.328
Al alloy	80.8 GPa	0.33
Epoxy resin	6.87 GPa	0.3

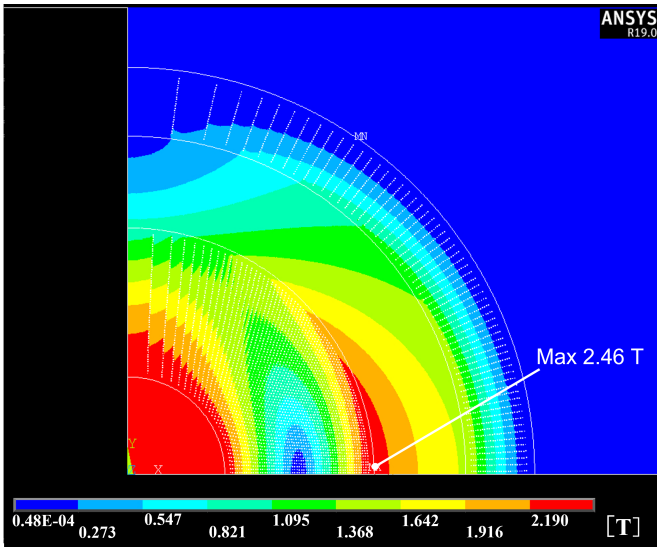


Fig. 4. Magnetic field distribution of the magnet cross-section in the first quadrant when the operating currents of the dipole coil and the active shielding coil are 217 A and 249 A, respectively.

## V. STRUCTURAL ANALYSIS

To investigate the effect of the EM force on the coil cross-section, a structural analysis of the magnet in two dimensions was conducted. The data of the EM force derived from the electromagnetic analysis described in section IV were used for the structural analysis. Fig. 5 and Fig. 6 show the displacement distribution and the stress distribution of the magnet under the EM force, respectively. The dipole coil is displaced in a radial direction toward the magnet center by the EM force. And the compressive stress generated in the dipole coil becomes larger near the midplane. The maximum stress in the dipole coil is  $14.8 \times 10^6$  Pa at the NbTi wire. In the shielding coil, the displacement increases as it approaches the midplane (x-axis), and the coil configuration extends outward on the x-axis.

Therefore, tensile stress is generated in the shield coil, and the stress becomes large especially around the mid-plane.

Regarding the supports of the shielding coil, the EM force generated in the shielding coil is mainly sustained with the outer support. Compared to the inner support and the shielding coil, therefore, a larger load is applied to the outer support. However, the load on the outer support is significantly smaller than the yield strength of 5083 Al alloy which is 178 MPa at 4 K. The inner support is hardly loaded by the EM force.

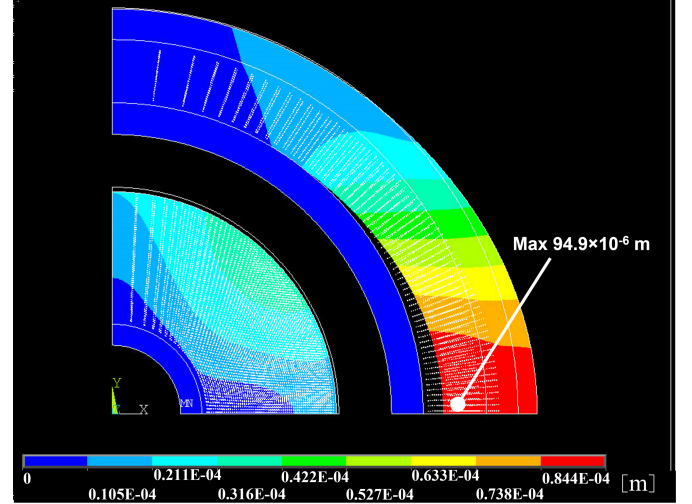


Fig. 5. Displacement distribution of the magnet cross-section in the first quadrant at the rated operation of the magnet.

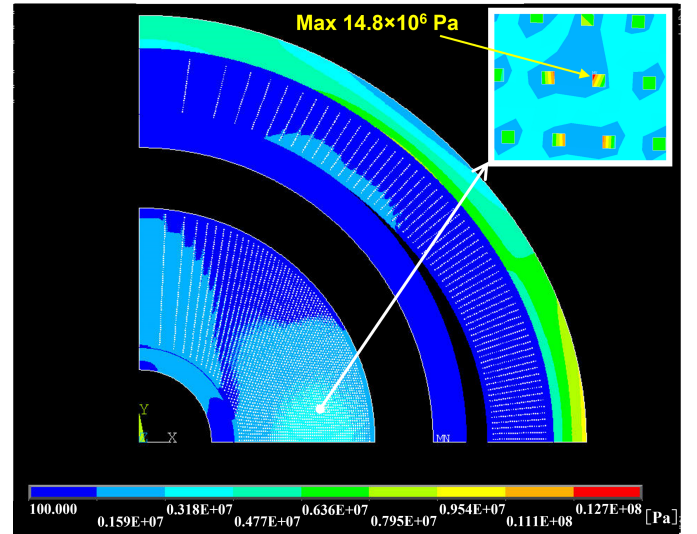


Fig. 6. Stress distribution of the magnet cross-section in the first quadrant at the rated operation of the magnet. The upper right frame shows an enlarged view of the part where the maximum stress is generated.

## VI. EVALUATION OF THE MAGNET WEIGHT

In the previous study [5], the weight of the magnet with active shielding was evaluated without taking into account the coil support's weight. In this study, the weight evaluation of the magnet, including the coil support, was conducted. The coil support is made of 5083 Al alloy the density of which is 2688 kg/m<sup>3</sup>. The details of the other components, except for



the coil support, are described in Ref [5]. Table 4 shows the weight per unit length for the magnet with active shielding and the magnet with an iron yoke. In the magnet with shielding coil, the epoxy resin for impregnating coil windings is the heaviest component. Also, the epoxy resin and the coil support make up most of the magnet weight. Comparing the weight of both magnets, the magnet with active shielding is one-third lighter than the magnet with an iron yoke. As a result, the active shielding technology can largely reduce the weight of superconducting magnets for a rotating gantry.

Table 4. Magnet weight per unit length for the magnet with active shielding and the magnet with iron yoke.

	Magnet with active shielding	Magnet with iron yoke
Dipole coil winding	79 kg/m	28 kg/m
Shield coil winding	34 kg/m	—
Iron yoke	—	2472 kg/m
Epoxy	380 kg/m	25 kg/m
Coil support	355 kg/m	—
Total weight	848 kg/m	2525 kg/m

## VII. DISCUSSION

In section V, the results of the structural analysis indicated that the cross-sections of the dipole and the shielding coils were deformed due to the EM force during the rated operation of the magnet. It is concerning that the coil deformation has a large effect on the field quality of the magnet. Therefore, the effect of the coil deformation on the field quality was investigated.

Multiple coefficients for the magnetic field before and after the coil deformation were compared at the reference radius of 60 mm. Table 5 shows the normal multipole coefficients of the designed and the deformed coil cross-sections, and the difference in the coefficients before and after coil deformation. The multipole coefficients are expressed in units normalized by the dipole field of the designed coil cross-section, which is not affected by the EM force. The multipole coefficients are evaluated with respect to the dipole field, which equals  $1.0 \times 10^4$  units.

Comparing the multipole coefficients before and after the coil deformation, there are slight differences in  $b_1$ ,  $b_3$ ,  $b_5$ , and  $b_7$ . However, the magnetic field quality of the deformed coil cross-section meets the design requirements described in Section II. As a result, the design concept of superconducting magnets with active shields is valid in terms of magnetic field and the support structure for a rotating gantry.

Table 5. The normal multipole coefficients of the designed and deformed coil cross-sections, and the difference in the coefficients before and after coil deformation.

Multipole coefficients	Designed coil cross-section (A) [Unit]	Deformed coil cross section (B) [Unit]	Difference between (A) and (B) [Unit]
$b_1$	10000.0	10001.7	1.7
$b_3$	-1.0	-0.6	0.4
$b_5$	0.3	0.4	0.1
$b_7$	0.0	-0.1	0.1

\*  $b_2$ ,  $b_4$ ,  $b_6$ , ...,  $b_{2n}$  are 0 unit because this FEM model is symmetrical.

## VIII. CONCLUSION AND FURTHER PLANS

An electromagnetic-structural analysis of a superconducting magnet with active shielding for a rotating gantry was conducted using an FEM model. The results of the analysis indicated that the peak field of the magnet is located at the outer section of the dipole coil, and the magnitude of the peak field is comparable with that of the dipole field in the magnet. The dipole coil is compressed in a radial direction toward the coil center by EM force, and the stress generated in the dipole coil becomes larger near the midplane. In the shielding coil, the EM force is mainly sustained with the outer support.

Based on the results of the analyses, the effect of the coil deformation due to EM force on the field quality was investigated. As a result, the coil deformation has a slight effect on the quality of the field quality but is negligible for the magnet operation.

In addition, the reevaluation of the magnet with an active shielding coil, including the coil support, was conducted while considering the previous study. The evaluation indicated that the magnet with active shielding is one-third lighter than the magnet surrounded with an iron yoke, in terms of the magnet weight per unit length.

As a further plan, the effects of the coil misalignment in the magnet assembly and the thermal stress generated during magnet cooling on the magnet performance are going to be investigated by using a two-dimensional cross-section model. Additionally, a three-dimensional design study is going to be conducted on superconducting magnets with active shielding. Using three-dimensional coil configurations, a leakage field from the magnet in the longitudinal direction will be evaluated. And quench protection of the magnet will be designed, based on coil inductance derived from the three-dimensional coil configuration.

## ACKNOWLEDGMENT

The author would like to thank Mr. T. Orikasa of Toshiba Energy Systems & Solutions Corporation for his technical supports.

## REFERENCES

- [1] Y. Iwata *et al.*, "Design of a superconducting rotating gantry for heavy-ion therapy," *Phys. Rev. ST Accel Beams*, vol.15, no.4, 2012, Art. ID 044701.
- [2] Y. Iwata *et al.*, "Development of a superconducting rotating-gantry for heavy-ion therapy," *Nucl. Instrum. and Meth. In Phys. Res.*, B 317, 2012, pp. 793-797.
- [3] S. Takayama *et al.*, "Design and Test Results of Superconducting Magnet for Heavy-Ion Rotating Gantry," IOP Conf. Series: JPCS. vol.871, 2017, Art. ID 012083.
- [4] T. Obana *et al.*, "Magnetic field and structure analysis of a superconducting dipole magnet for a rotating gantry," *Physica C*, vol.471, 2011, pp. 1445-1448.
- [5] T. Obana *et al.*, "Design of Lightweight Superconducting Magnets for a Rotating Gantry With Active Shielding," *IEEE Trans. Appl. Supercond.*, vol.30, no.4, 2020, Art. ID 4400305.
- [6] N. Amemiya *et al.*, "Measurements of Magnetic Field Harmonics In Superconductor Coil Wound By Surface Winding Technology," *IEEE Trans. Appl. Supercond.*, vol.22, no.3, 2012, Art. ID 9000404.

- [7] T. Obana *et al.*, "Prototype superconducting magnet for the FFAG accelerator," *Fusion Eng. Des.*, vol.81, 2006, pp. 2541-2547.
- [8] T. Obana *et al.*, "Magnetic Field Design of a Superconducting Magnet for a FFAG Accelerator," *IEEE Trans. Appl. Supercond.*, vol.15, no.2, 2005, pp. 1185-1188.
- [9] ANSYS 19, <https://www.ansys.com>